Universidad de Granada
FisyMat

a Book

of Fascinating Facts

William Schoenell

Advised by: Narciso Benítez

Table of Contents

1 Introduction **1**
- 1.1 Surveys . . . 1
- 1.2 The ALHAMBRA survey . . . 1
- 1.3 The S-PLUS survey . . . 1
- 1.4 The J-PAS survey . . . 2

2 The southern A-PLUS telescope **5**
- 2.1 T80S installations . . . 5
  - 2.1.1 Telescope . . . 5
  - 2.1.2 Instrument . . . 6
  - 2.1.3 Enviroment monitoring . . . 7
  - 2.1.4 Data center . . . 7
  - 2.1.5 Chimera: The T80S OCS . . . 7

3 BLABLABLA **9**
- 3.1 Motivation . . . 9
- 3.2 Notation . . . 11
- 3.3 Bayesian photometric redshifts: The BPZ method . . . 11
- 3.4 From redshift PDFs to stellar properties PDFs . . . 13
- 3.5 Algorithm . . . 15
- 3.6 Stellar mass estimates . . . 17
- 3.7 Validation of the SED fitting . . . 17
  - 3.7.1 Simulations . . . 17
  - 3.7.2 Effects of the reddening law . . . 17
  - 3.7.3 Comparison w/Taylor . . . 17

4 Application ... the Mass function - alhambra **19**
- 4.1 V_{MAX} PDF . . . 19

5 Random toughts **21**

6 Conclusions and Further work **23**

Bibliography **25**

Chapter One

Introduction

Say about the importance of measuring galaxies properties.

Emphasis on narrow band surveys like from Benítez et al. (2009):

```
As Hickson et al. (1994) first showed, multiband narrow filters can
 be much more efficient than spectroscopy for ob-
taining redshifts if the large area of the imaging cameras is factore
Several photometric surveys, using different fil-
ter systems, have been proposed or implemented in the last decade: th
 UBC-NASA survey (Hickson & Mulrooney 1998),
 CADIS (Wolf et al. 2001b), COMBO-17 (Wolf et al. 2001a), COSMOS-21
 (Taniguchi 2004), Advanced, Large, Homoge-
  neous Area, Medium Band Redshift Astronomical (ALHAM- BRA; Moles et
   DES (DES Collaboration 2005), LSST
   (Tyson 2006), PanStarrs (Kaiser 2007), VST (Arnaboldi et al. 2007)
   and PAU (Benitez et al. 2009). These surveys repre-

sent powerful alternatives to deep spectroscopic surveys such as DEEP
(Davis et al. 2003), VVDS (Le Fe‘vre et al. 2003),
 or BOSS (Schlegel et al. 2007) at least for those scientific goals w
 require limited redshift accuracy and low
 -resolution spectral information.
```

1.1 Surveys

1.2 The ALHAMBRA survey

Explain figure 1.1

1.3 The S-PLUS survey

Explain figure 1.2

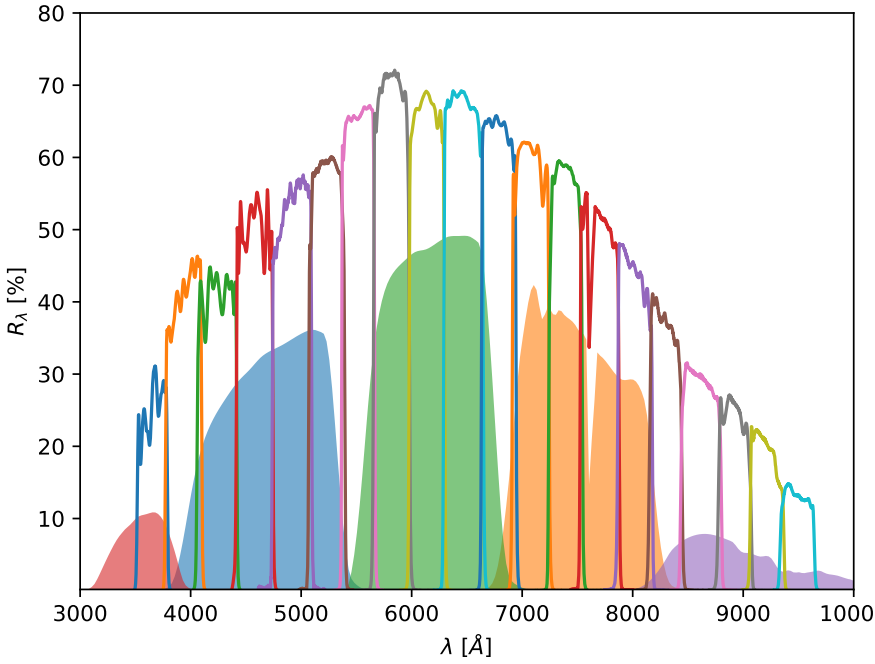

From Benítez (2000). This is a figure, simple and poorly drawn by my computer. The lines, intended to be physical representations of the glittering abstraction of pure length, have come out wobbly, like a plum pudding with too much plum. I will send my computer back to arithmetic class. FIGURE 1.1

1.4 The J-PAS survey

Explain figure 1.3

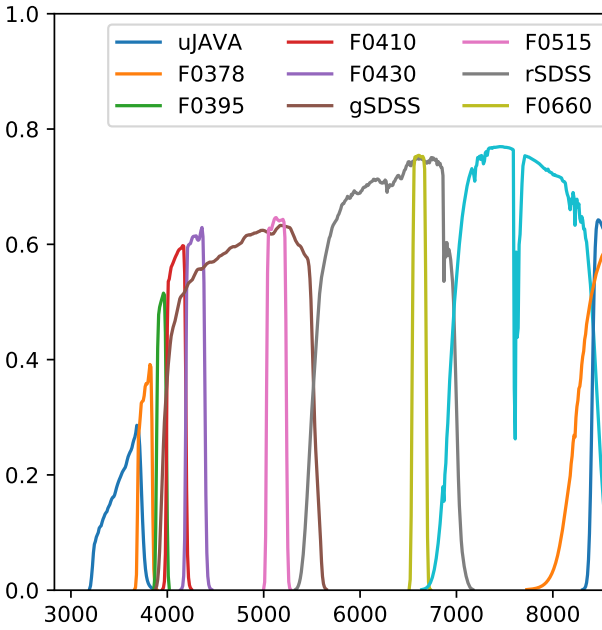

FIGURE 1.2 From Benítez (2000). This is a figure, simple and poorly drawn by my computer. The lines, intended to be physical representations of the glittering abstraction of pure length, have come out wobbly, like a plum pudding with too much plum. I will send my computer back to arithmetic class.

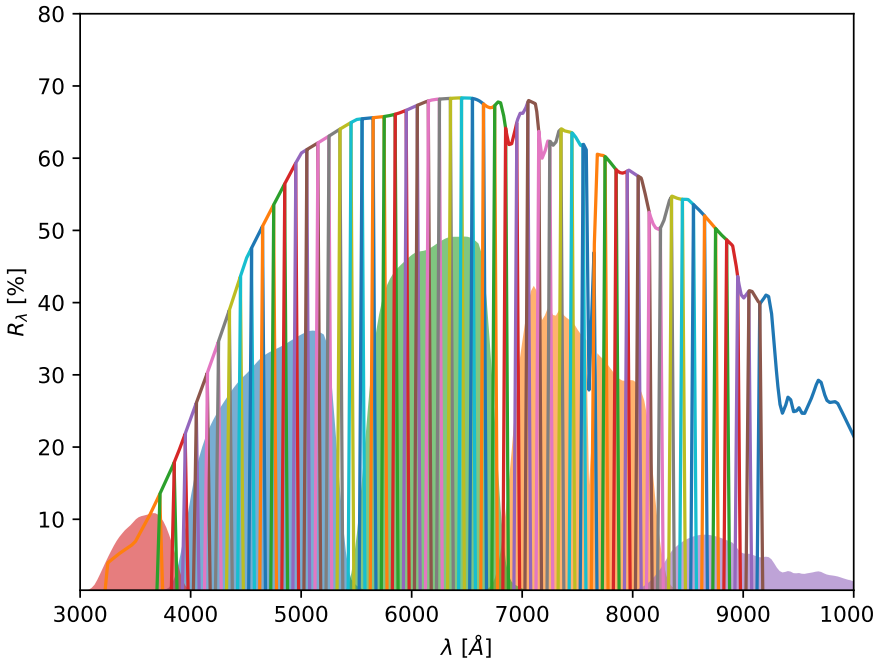

From Benítez (2000). This is a figure, simple and poorly drawn by my computer. The lines, intended to be physical representations of the glittering abstraction of pure length, have come out wobbly, like a plum pudding with too much plum. I will send my computer back to arithmetic class.

FIGURE 1.3

Chapter Two

The southern A-PLUS telescope

In this chapter we describe the design and the installation of the Brazilian counterpart of the 86 cm telescope installed on Teruel. The T80S telescope is a **improve this** founded project by the Brazilian institutions IAG, ON and LNA. The main objective for building the telescope is to carry two surveys the A-PLUS and the S-POL. The A-PLUS will be a photometric survey on the southern hemisphere **meter figura da area** on twelve optical filters **TODO meter tabela e curavs**. The S-POL (tbd).

2.1 T80S installations

The T80-South telescope is situated near the summit of Cerro Tololo in central Chile, at an altitude of 2,207 m, at latitude -30:10:10.78 and longitude -70:48:23.49. It is installed on a small building with the dome, a small data center for data processing and two auxiliary rooms for instrument engineering purposes. The operation of the telescope is designed to be fully automated and it is controlled by the observatory control system (OCS) developed by our team **explain better** since 2008. More details of the OCS will be described on 2.1.5.

2.1.1 Telescope

The T80S is a new generation of Ritchey-Chretien Cassegrain telescopes with a huge field of view (FoV) of 2 square degrees. The design of telescopes with such FoVs are crucial to conduct astromical surveys as it allows to cover huge areas on the sky with relatively small amounts of time. The telescope design was developed by Advanced Mechanical and Optical Systems (AMOS) in Liège, Belgium with the mechanical fabrication, assembly and control systems subcontracted to the German company ASTELCO Systems GmbH in Munich. The telescope control is done via a private protocol called OpenTPL developed by Tau-Tec GmbH. More details on the control of the telescope are explained on section 2.1.5.

The telescope detailed optical parameters are shown on table 2.1.1.

Primary Mirror (M1)	
Curvature radius	-2471.295mm concave
Conic constant	$-1.163\,946$
Optical Diameter	826mm
Central hole	**TODO**
Used clear aperture	**TODO**
Effective collecting area	0.44m^2
Secondary F/4.5 mirror (M2)	
Distance from Primary	825.7695mm
Radius of curvature	-1237.411mm convex
Conic constant	$-5.776\,745$
Optical Diameter	302.879mm

T80S telescope optical specifications

The alignment of the secondary mirror with respect of the primary mirror needs to be done on each pointing due the large FoV area. The telescope center of mass and temperature changes the alignment, so a simple model was implemented by

2.1.2 Instrument

On both photometric and polarimetric mode, T80S will use a Spectral Instruments 1100S camera equipped with an E2V 290-99-1-F24 CCD (serial number 11323-24-01). This CCD is mounted on the focal plane with a filter+shutter unit (FSU) **figure here!** between it and the telescope flange. The filter shutter unit is composed of a custom-made shutter by Bonn Shutters and filter wheels with their motors and encoders according the observation model (polarimetric or photometric).

The mechanical part of the FSU was designed at Instituto de Pesquisas Espaciais, in Brazil, and produced by MetalCard. The control of the FSU was designed by another Brazilian company Solunia using Programable Logic Controllers PLCs from Beckhoff.

On the photometric mode, the FSU counts with two filter wheels with 7 positions each (6 filters plus 1 clear position) and it also hosts a guiding camera at the border of the focal plane which is not used at the moment since the telescope tracking is sufficiently accurate for the exposure times of the survey **cite table survey exposure times**.

TODO: EXPAND ON THIS On the polarimetric mode, the FSU counts with one filter wheel, one polarimetric wheel which spins a crystal of calcite, giving the required polarization phase for each exposure and one ???

Router	
Curvature radius	−2471.295mm concave
Effective collecting area	0.44m^2
Switch	
Distance from Primary Application APP	825.7695mm
Conic constant	−5.776 745
Optical Diameter	302.879mm

TABLE 2.2 T80S data center hardware specifications

2.1.3 Enviroment monitoring

2.1.4 Data center

The data center was designed to store the brute data from the observations and to have the computing capacity to reduce online the data which is being acquired by the camera. It is located on the Technical Room on figure **figure map telescope**.

Having the pipeline being executed online together with the observations facilitate the survey scheduling, making decisions that minimizes the survey time minimizing the number of fields that must be re-visited.

The data center counts with one router and one switch for network communications together with 5 servers: three application servers (APP), one camera server (CAM) and one storage server (STO). There is a sixth server which is located on La Serena city, at CTIO headquarters, which will store the data backup. An detailed list of hardware is shown on table 2.1.4

2.1.5 Chimera: The T80S OCS

Every operation of the T80S telescope is controlled by a fully-distributed software called chimera[1]. Developed in Python, it uses Python Remote Objects[2] as technology to distribute objects across the different computers and operational systems. Since its dependencies are very low, chimera haves the advantage to run on many flavours of operational systems such Windows, Linux and even Andriod letting the implementations be easily ported from one architecture to another one.

Chimera is designed in three main layers:

- Core: The core of chimera holds all the common methods for all chimera modules such as low end communication methods to

[1] http://github.com/astroufsc/chimera/
[2] http://www.pythonhosted.org/Pyro/

translate PYRO objects into chimera objects and basic astronomical-related methods like coordinates conversions and file names creations and events control

- Instrument drivers provide the abstraction from the hardware particular characteristics implementing common methods across all the instruments of a specific type. With this approach, every instrument haves a common inteface with methods and events which some are mandatory and some optional. For example, for a Telescope method, a
- Controllers are the high level interfaces operating on the instruments through their standard methods to do all the inherent tasks to an astronomical observatory.

Chapter Three

A method to measure stellar properties of galaxies from redshift templates

In this chapter we introduce a new method which combines the output of a bayesian photometric redshift code with a stellar population analysis to estimate basic galaxy properties, with emphasis on its stellar mass $M_\star$. The method is applicable to any set of photometric data, but we apply it to the ALHAMBRA filter set. The next chapter applies the method to construct the stellar mass function of the ALHAMBRA survey.

3.1 Motivation

The main motivation of the work described in this chapter is to have a robust method for determining stellar masses ($M_\star$) out of photometric data alone, without relying on any spectroscopic information. As explained in the introduction to this thesis, photometric surveys like DES (REF), JPAS (REF), LSST (REF) and many others are one of the main sources of data for observational cosmology and extragalactric astrophysics nowadays. Most of these mega-surveys aim to use the data to estimate galaxy redshifts and address cosmological questions like the nature of dark energy. However, it would certainly be positive/smart to use these same data to learn more about galaxies than their "mere" redshifts. This is the central motivation of the work presented in this chapter.

Many previous studies used photometry to estimate $M_\star$, like Taylor et al. (2011), Brinchmann et al. (2004), REFS..... All of these, however, make use of a spectroscopic z to map the observed filter on the galaxy frame and to calculate the objects luminosity, which is then combined with a stellar mass-to-light ratio to determine $M_\star$. Taylor et al. (2011), for instance, builds an extensive library of model galaxy spectra, from which synthetic magnitudes are computed to be then compared to the SDSS DR7 u, g, r, i and z optical filters, but the distance, which is the main ingredient to calulate the galaxy luminosity, is derived from very accurate spectroscopic redshifts obtained both with SDSS and AAOmega spectrographs with very precise redshifts measurements which are described on sec 2.1 of Taylor et al. (2011).

This approach needs to be modified when spectroscopic redshifts are not available. In general terms, one now need to simultaneously estimate both the stellar population properties and the redshift out of photometric data alone.

This is done, for instance, by ??REF??, where !!!! BLABLABLA. Other studies in this same general line of work include REF, REF, and REF. MUFFIT ? fits two old SSPs using the redshift from BPZ as input (Le Phare ?) (CIGALE needs the redshift) (HYPERZ haves a mass option but I do not have details on how it works)... To be expanded...

In this work we separate the task of estimating z from that of estimating $M_\star$ and other stellar population properties. In broad lines, the method works as follows:

1. applies a photo-z code to a photometric dataset D to obtain $p(z, T)$, the probability that a galaxy is at redshift z and is described by a spectral template T
2. fits the template spectra in terms of stellar population models, obtaining, the probability $p(\theta|z, T)$ of a given property θ (e.g., the mass-to-light ratio) for fixed z and T
3. applies a "template expansion" to combine the photo-z PDF with the stellar property PDF to obtain $P(\theta|D)$, the probability of property θ given the data D

The main advantages of this method in comparison with the other mentioned methods are:

1. it restricts parameter space to colors of real Universe galaxies
2. by applying the "template expansion", we avoid the problem of dealing with emission lines of galaxies and only focus on the stellar population content of them **Random tought: Can someone ask me about nebular continuum here?**
3. as will be shown, once the stellar population parameter PDF $p(\theta|z, T)$ is calculated for a set of filters and stellar population models, calculating any galaxy stellar parameters is just a matter of combining $p(\theta|z, T)$ with the galaxy's redshift PDF $p(z, T|D, I)$
4. although we are applying our method to the ALHAMBRA survey as a test case, the non-dependence of spectral redshifts makes our method applicable to larger datasets and will enable us to have robust stellar masses probability distribution functions to any photometric redshift survey such as DES and JPAS

TODO: explain content of each section of this chap below ... We start by describing the BPZ code of Benítez (2000) on section 3.3 and on section 3.4, we introduce our method to derive the stellar populations parameters from the output redshift probability distribution functions (PDFs).

3.2 Notation

For clarity, let us introduce in this section the concepts involved on the redshift and galaxy property estimation and establish their notations.

- θ: parameters
- $M_\star$: galaxy stellar mass
- $S_{k,l}$: Magnitude of stellar population model k on filter l.
  $S_{k,l} = -2.5 \log\left(\frac{\int_l F_k^{CSP} R_\lambda \lambda d\lambda}{\int_l R_\lambda \lambda^{-1} d\lambda}\right)$, following eq. 2 of **?**.
- ...

3.3 Bayesian photometric redshifts: The BPZ method

Photometric redshifts are the cheapest and fastest way for the determination of the distance of galaxies. The precision of these distances is undeniably smaller that the spectroscopic ones but the number of galaxies that can be covered with the same amount of telescope time and the use of the redshift probability distribution functions (PDFs) are shown to be very powerful when the goal is to have a statistical sample.

Also it was shown by many authors **from sheldon 2012: (Mandelbaum et al. 2008; Cunha et al. 2009; Wittman 2009; Bordoloi et al. 2010; Abrahamse et al. 2011)** that using a simple estimator like the maximum likelihood or the likelihood average leads the results to significant biases so any method that rely on photometric redshifts should take in account the full probability distribution function.

For the photometric redshift calculations, we use the bayesian photometric redshift code BPZ (Benítez, 2000). BPZ calculates the probability distribution function (PDF) of the objects being on a redshift z_i and of a spectral type T_j.

The probability $p(z_i, T_j|D, I)$ for z_i to be the true redshift and T_j be the spectral type of a given observed galaxy with N_l observed fluxes/magnitudes ($D = m_l$, or more conveniently $D = \vec{C}, m_0$ where $\vec{C} = \{m_1 - m0, m_2 - m_0, \ldots\}$ represent the colors between an apparent magnitude m_0 and the others) can be written as:

$$p(z_i, T_j|\vec{C}, m_0, I) = \frac{p(\vec{C}, m_0|z_i, T_j, I) \times p(z_i, T_j|I)}{p(\vec{C}, m_0|I)} \tag{3.1}$$

which comes directly from Bayes theorem. The left side of the equation is called hypothesis and, on the right side, we have the redshift likelihood times the prior on the numerator and the denominator is the evidence. Since we are just interested on the estimation of the redshift, the evidence turns into an ordinary normalization constant (Sivia and Sikilling, 2006).

The redshift likelihood $p(\vec{C}, m_0|z_i, T_j, I)$ can be written as:

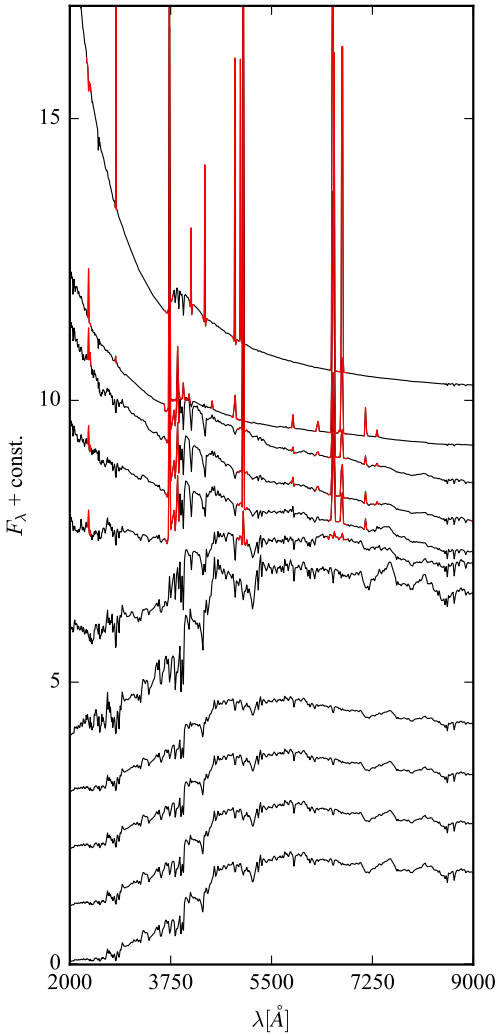

aa

$$p(\vec{C}, m_0|z_i, T_j, I) = e^{-\frac{\chi^2_{ij}}{2}} \tag{3.2}$$

where χ^2 is given by the sum over all photometric filters $l = 1, \ldots N_l$ of the quadratic difference between the i-th template to the observed flux f^T_{ij} or magnitude m^T_{ij}.

So, in case of the χ^2 in fluxes, we have:

$$\chi^2_{i,j} = \sum_l \left({f_l^O}^2 - a_{i,j} {f^T_{l,i,j}}^2 \right) w_l^2 \tag{3.3}$$

where a is a template normalization factor which can be calculated by minimizing the χ^2 value. The w_l is a weight factor which is essentially dependent of the error in the observed magnitude, e.g. $w_l = \frac{1}{\sigma_l}$. [1]

It can be easily shown that for magnitudes this scaling factor a_j becomes an additive factor, making the magnitude χ^2 in the form:

$$\chi^2_{i,j} = \sum_l \left(m_l^O - m^T_{l,i,j} + A_{i,j} \right)^2 w_l^2 \tag{3.4}$$

The first term on the right side of the equation 3.1, the template-redshift prior, is used to modulate the evidence in the form that unrealistic template, redshift and apparent magnitude combinations are less taken in account than more realistic ones. In pratice, two effects are taken in account on this prior: galaxies cannot be too far if they are too bright (i.e. low apparent magnitude m_0) and galaxies average colors must be slightly bluer as redhifts increases.

On figure 3.2, taken from Benítez (2000), the two effects are shown. From top to bottom, on the first panel, we have an example of what would be a redshift likelihood for the different spectral types. On the second panel, the prior is shown with the characteristics metioned before and, on the third and fourth panels the final redshift PDF. Note that if a flat prior were assumed, the most likely redshift for the galaxy would be around 2.8 but, after applying the prior distribution, this peak goes back to around 0.3.

This prior distribution is empirically calibrated using colors and spectroscopic redshifts for the Hubble Deep Field North. For more details on the empirical redshift prior distribution, we invite the reader to give a look on Benítez (2000).

3.4 From redshift PDFs to stellar properties PDFs

Given a stellar population spectrum S_k which is a spectrum composed by a model with $\vec{\theta}_k$ set of parameters, one can write the probability of

[1] This weight can be changed to accommodate, for example, templates with intrinsic errors, error scaling factors, etc...

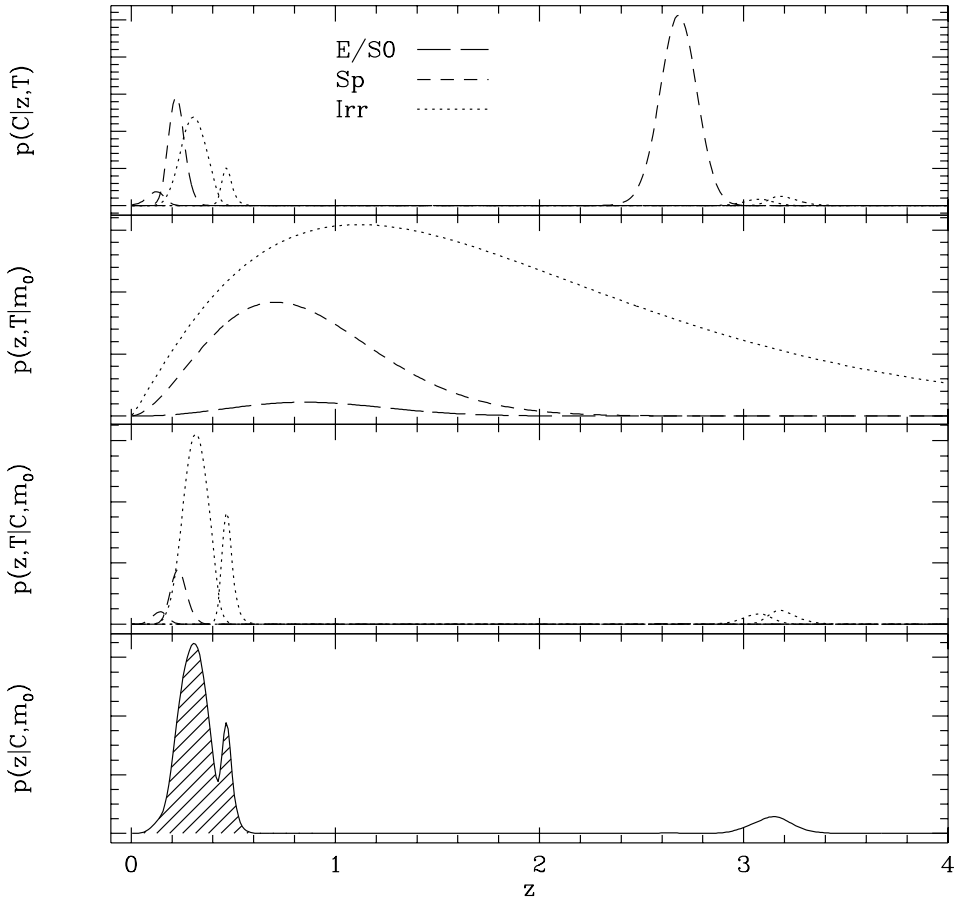

From Benítez (2000). This is a figure, simple and poorly drawn by my computer. The lines, intended to be physical representations of the glittering abstraction of pure length, have come out wobbly, like a plum pudding with too much plum. I will send my computer back to arithmetic class.

FIGURE 3.2

the parameters be the parameters that reproduce the galaxy colors $\vec{C}$ and apparent magnitude m_0 as:

$$p(\vec{\theta}_k|\vec{C}, m_0) \tag{3.5}$$

if we want to, at the same time, calculate the PDF of the same galaxy to have stellar properties $\vec{\theta}_k$, redshift z_i, we can write the equation in the form:

$$p(\vec{\theta}_k, z_i|\vec{C}, m_0) = \sum_{j=1}^{N_T} p(\theta_k, z_i, T_j|\vec{C}, m_0) \tag{3.6}$$

applying the chain rule on the right term, we can open the term inside the sum as:

$$p(\vec{\theta}_k, z_i, T_j|\vec{C}, m_0) = p(z_i, T_j|\vec{C}, m_0)p(\vec{\theta}_k|z_i, T_j, \vec{C}, m_0) \tag{3.7}$$

Since there is no dependence on $\vec{C}, m_0$ with $\vec{\theta}_k$, we rewrite the equation as

$$p(\vec{\theta}_k, z_i, T_j|\vec{C}, m_0) = p(z_i, T_j|\vec{C}, m_0)p(\vec{\theta}_k|z_i, T_j) \tag{3.8}$$

where $p(z_i, T_j|\vec{C}, m_0)$ is the template-redshift probability distribution function given by BPZ (or any other probabilistic photometric redshift code) which is described on section 3.3 and the stellar population PDF is given by

$$p(\vec{\theta}_k|z_i, T_j) \propto p_I(\vec{\theta})p(T_j|\vec{\theta}_k, z_i) \tag{3.9}$$

Assuming a flat prior will incur that the prior will be dominated by the sampling on $\vec{\theta}_k$ space, therefore $p_I(\vec{\theta}_k) = \delta\vec{\theta}_k$ and the likelihood defined by:

$$p(T_j|\vec{\theta}_k, z_i) = \mathcal{L}_{i,j,k} = \exp\left(\frac{1}{2}\sum_l \left(m_k^S - m_{i,j}^T + A_{i,j,k}\right)^2 w^2\right) \tag{3.10}$$

where $A_{i,j,k}$, as mentioned on sec. 3.3 is a mere minimization constant and, for our pourposes, will be neglected as it haves no practical meaning. $w = \frac{1}{\epsilon}$ is an ad-hoc term introduced to modulate the intrinsic error floor between the stellar population model and the photo-z template. Different ϵ factors were tested on the simulations done on 3.7.1 and a value of $\epsilon = 0.05$ mag was adopted (the same is adopted on Taylor2011)

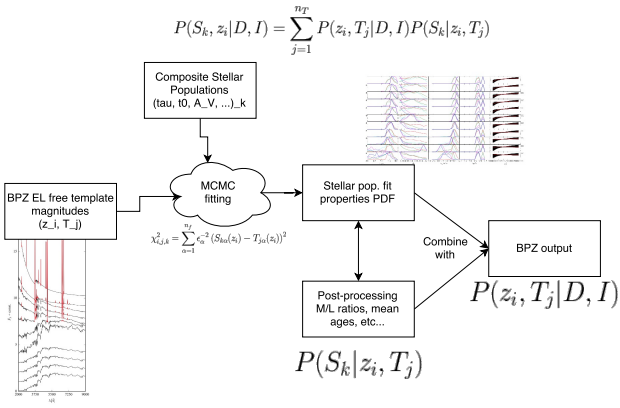

aa

Parameter	Units	min/max values	Description
t_0	yr	1×10^6 to t_U	Age of the exponential burst. t_U is the age of Universe at z
θ		0.1 to 10	$\theta = \tau \times t_0$. τ is burst e-folding time
Z	$Z_\odot$	$0.2, 0.4, 1, 1.5$	Stellar metallicity
A_V	mag	-0.1 to 2	Extinction in V-band (Cardelli et al., 1989, reddening law)

Synthetic CSP library parameters priors and descriptions TABLE 3.1

3.5 Algorithm

To describe in a more practical way, we arranged all the steps involved on the estimation of the stellar properties such as stellar mass of a galaxy with a template-redshift PDF $p(z_i, T_j|\vec{C}, m_0)$.

The pre-processing steps on the BPZ templates done are:

1. Remove BPZ emission lines: To compare stelllar population models with BPZ templates, the BPZ emission lines must be removed. On figure 3.1 we draw the 11 BPZ templates marking in red the emission lines that were removed from spectra.

2. Interpolate BPZ templates: The emission line free templates are lineary interpolated between them 3 times as it is done on BPZ so, for each redshift bin, there is 41 templates.

3. For each (i, j) pair on the template-redshift space, evaluate the template magnitudes $m^T_{i,j}$ for the filters of the survey we are going to measure the properties.

The BPZ template magnitudes $m_{i,j}^{T}$ are fitted by a set of random composite stellar populations defined by the parameters listed on table 3.5 where we list the parameter names and descriptions, units and values allowed by the fit of the stellar populations. The simple stellar populations library used to make the composite stellar populations was (Bruzual and Charlot, 2003, BC03) with **cite Chabrirer IMF and Padova1994 stellar tracks**. We chose boundary values that are very similar to e.g. Taylor et al. (2011) and Brinchmann et al. (2004) and many others. It is not our goal on this work to test many different spectral libraries here but the effectiveness of the method itself on recovering basic stellar population properties.

We also used only the 20 optical filters of the ALHAMBRA survey (see fig 1.1), neglecting the three near-IR ones. This is another simplification that is based on the lack of good stellar population models on the IR **EXPAND!!** and see sec. 4 of (Taylor et al., 2011).

There is not an unique approach for estimating $p(\vec{\theta}, z_i|\vec{C}, m_0)$. The most simple one would be construct a fine grid on the model space but most of the mathematically possible models are not physical, so a smarter parameter space should was developed. For that we used the emcee code (Foreman-Mackey et al., 2013) to map the probability space on regions where the probability is not so negligible. The emcee[2] code is a Python code that implements the affine-invariant ensamble sampler for Markov Chain Monte Carlo (MCMC). We randomly initialize 70 walkers and sample the parameter space looking for a set of most probable likelihoods. To achieve that, we run each walker for 3000 steps, removing the first 1000 steps as burn-in phase. Visual inspection of the chains was done to make sure this burn-in phase was met.

Things that I am not describing nowhere and still don't know where describe it:

1. The magnitude eq for λ. Explain that I am counting photons and bla bla.

2. How a CSP spectra is formed

3.6 Stellar mass estimates

3.7 Validation of the SED fitting

In this section we show some results of simulations to determine how precise one can infer galaxies properties for a given set of magnitudes within the chosen filter set and

[2] https://github.com/dfm/emcee

3.7.1 Simulations

effects of ϵ ,...

3.7.2 Effects of the reddening law

3.7.3 Comparison w/Taylor

Chapter Four

Application ... the Mass function - alhambra

4.1 V_{MAX} PDF

Chapter Five

Random toughts

?????? The survey selection functions of photometric surveys are usually much simpler than of the spectroscopic surveys, facilitating the account for selection biases on stellar and luminosity function easier. ??????

Chapter Six

Conclusions and Further work

Bibliography

Benítez, N.: 2000, *ApJ* **536**, 571

Benítez, N., Moles, M., Aguerri, J. A. L., Alfaro, E., Broadhurst, T., Cabrera-Caño, J., Castander, F. J., Cepa, J., Cerviño, M., Cristóbal-Hornillos, D., Fernández-Soto, A., González Delgado, R. M., Infante, L., Márquez, I., Martínez, V. J., Masegosa, J., Del Olmo, A., Perea, J., Prada, F., Quintana, J. M., and Sánchez, S. F.: 2009, *ApJ* **692**, L5

Brinchmann, J., Charlot, S., White, S. D. M., Tremonti, C., Kauffmann, G., Heckman, T., and Brinkmann, J.: 2004, *MNRAS* **351**, 1151

Bruzual, G. and Charlot, S.: 2003, *MNRAS* **344**, 1000

Cardelli, J. A., Clayton, G. C., and Mathis, J. S.: 1989, *ApJ* **345**, 245

Foreman-Mackey, D., Hogg, D. W., Lang, D., and Goodman, J.: 2013, *PASP* **125**, 306

Sivia, D. and Sikilling, J.: 2006, *Data Analysis: A Bayesian Tutorial*, Oxford University Press, 2nd edition

Taylor, E. N., Hopkins, A. M., Baldry, I. K., Brown, M. J. I., Driver, S. P., Kelvin, L. S., Hill, D. T., Robotham, A. S. G., Bland-Hawthorn, J., Jones, D. H., Sharp, R. G., Thomas, D., Liske, J., Loveday, J., Norberg, P., Peacock, J. A., Bamford, S. P., Brough, S., Colless, M., Cameron, E., Conselice, C. J., Croom, S. M., Frenk, C. S., Gunawardhana, M., Kuijken, K., Nichol, R. C., Parkinson, H. R., Phillipps, S., Pimbblet, K. A., Popescu, C. C., Prescott, M., Sutherland, W. J., Tuffs, R. J., van Kampen, E., and Wijesinghe, D.: 2011, *MNRAS* **418**, 1587